Synthesis, Nanostructure, Functionality, and Application of Polyfluorene−block−poly(N-isopropylacrylamide)s

ARTICLE *in* MACROMOLECULES · OCTOBER 2009

Impact Factor: 5.8 · DOI: 10.1021/ma9019619

282 *Macromolecules* **2010**, *43*, 282–291
DOI: 10.1021/ma9019619

Macromolecules
ARTICLE

Synthesis, Nanostructure, Functionality, and Application of Polyfluorene-*block*-poly(*N*-isopropylacrylamide)s

Yanqing Tian,*,†,§ Ching-Yi Chen,† Hin-Lap Yip,† Wen-Chung Wu,† Wen-Chang Chen,‡ and Alex K.-Y. Jen*,†

†*Department of Materials Science and Engineering, Box 352120, University of Washington, Seattle, Washington 98195-2120, and* ‡*Department of Chemical Engineering, National Taiwan University, Taipei, Taiwan 106.* §*Current address: Center for Ecogenomics, The Biodesign Institute, Arizona State University, Tempe, AZ 85287-5001.*

Received September 2, 2009; Revised Manuscript Received October 6, 2009

ABSTRACT: A series of amphiphilic rod−coil diblock copolymers with a polyfluorene (PF) as a hydrophobic and light-emitting rod and a poly(*N*-isopropylacrylamide) (PNIPAAm) as a hydrophilic coil were prepared. Their micellar nanostructures and fluorescence properties were stimulated using solvents, e.g., water and tetrahydrofuran (THF)/toluene (1:10 by volume), which were characterized using dynamic light scattering (DLS), transmission electron microscopy (TEM), atomic force microscopy (AFM), and fluorescence spectroscopy. A typical block copolymer **P2** (M_n = 14 400, M_w/M_n = 1.80, the PF weight fraction is 9.4%) in water exhibited micelles with the PNIPAAm block as the corona, whereas the polymer showed inverse micelles in mixed organic solvents of THF/toluene with PF as the corona. Such different nanostructures resulted in their different fluorescence properties. The fluorescence spectrum of **P2** did not indicate aggregations of the PF chains in the THF/toluene mixture. Blue emission with a high quantum yield (0.80) was observed. In contrast, strong aggregations of the PF chains were observed in the aqueous solution, resulting in low quantum efficient (0.26) fluorescence. These results clearly demonstrated that the functionality of the **P2** could be tuned through the solvent stimuli. The micelles of **P2** were further used as nanocarriers to load a water-insoluble tetrakis(mesityl)porphyrin ($H_2(Me_3)TPP$) into its micellar aqueous solution. Efficient fluorescence resonance energy transfer (FRET) between the PF (donor) and $H_2(Me_3)TPP$ (acceptor) (as high as 98% quenching of donor emission) was observed in their micellar solutions. Moreover, FRET contributes significantly to the efficiency of singlet oxygen generation from $H_2(Me_3)TPP$ molecules (with an efficiency factor of 2 as compared to non-FRET micelles). This study provided a feasible way to enable the application of water-insoluble porphyrin in aqueous solution and enhance its singlet oxygen generation efficiency.

Introduction

Rod−coil block copolymers with conjugated polymers/oligomers as the rod portion are considered as new nanostructured functional materials because they exhibit interesting morphologies of honeycomb, cylindrical, and nanowire structures as well as electrical and optical properties.[1] Some recent studies in this field have shifted their gravities to create one-, two-, or three-dimensional confinement of the functional moieties with desirable microphase-separated structures with nanometer periodicity to effectively affect the optical or electronic properties.[1a,1g,1h] Thus, the synthesis and investigation of new rod−coil block copolymers with well-ordered nanostructures are necessary and important. Furthermore, it is quite challenging to understand the modulation of their morphologies through a stimulus such as temperature, solvent, and pH value and the relationship between the functionality and nanostructure. Polyfluorene (PF)[2,3] is a conjugated polymer, widely studied as a blue emitter and biosensor. PF-containing block copolymers[1d,1i−1k,4,5] have been reported and were investigated as new block copolymers exhibiting fibrillar and spherical morphologies[1k] and stable blue-light-emitting materials in the organic light-emitting diodes.[1d,11] More recently, a few coil−rod−coil triblock copolymers[5] with the PF as the hydrophobic segment and a poly(*N*-isopropylacrylamide) (PNIPAAm) block as the temperature-stimulated hydrophilic/hydrophobic chain were synthesized, and the thermal responsive morphologies around the lower critical solution temperature (LCST)[6] of the PNIPAAm polymers were investigated.

On the other hand, porphyrin and its derivatives are a class of typical photosensitizers and widely used as drugs for photodynamic therapy (PDT) to treat keratosis, esophageal tumors, lung cancer, and bladder carcinoma.[7] Under light irradiation, the photosensitizer is excited to reach its singlet state, and then intersystem crossing of the photosensitizer to its triplet state occurs. In the presence of molecular oxygen, the photosensitizer further transfers its triplet state energy to nearby oxygen molecules to form reactive oxygen species, such as the singlet oxygen ($^1O_2$) or free radicals, and in the meantime, the photosensitizer returns to its ground state and the generated highly active $^1O_2$ will kill the tumors around it. PDT efficacy is strongly related with its photoactivity and singlet oxygen generation efficiency. However, as with other photosensitizing agents, many porphyrins have poor solubility in water and tend to aggregate in aqueous solutions, resulting in a loss of photochemical activity in biological environment.[8] To alleviate the above problems, one can encapsulate porphyrins into micelles or vesicles generated by

*To whom all correspondence should be addressed: Tel +1-480-965-9601, Fax +1-480-727-6588, e-mail yanqing.tian@asu.edu (Y.T.); Tel +1-206-543-2626, Fax 206-543-3100, e-mail ajen@u.washington.edu (A.K.-Y.J.).

 Published on Web 10/26/2009

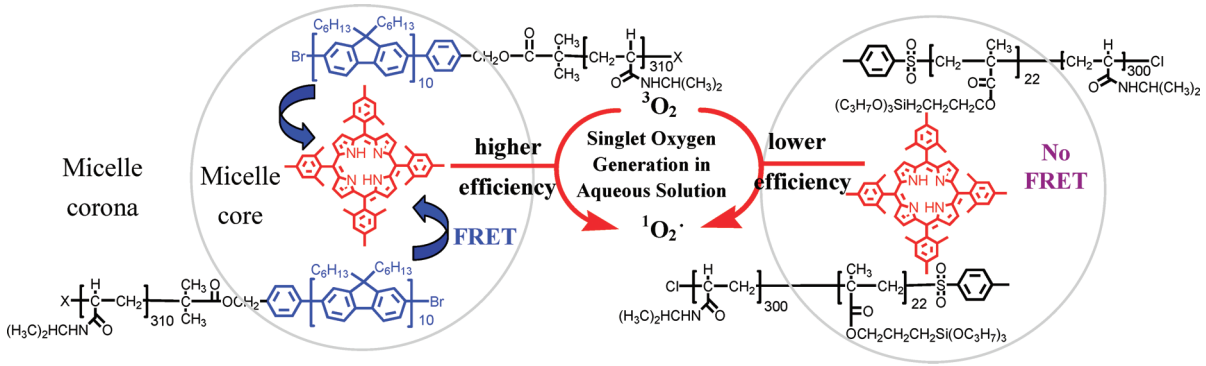

Figure 1. Schematic drawing of the utilization of the block copolymers to incorporate the $H_2(Me_3)TPP$ into their micellar cores and the enhancement of the singlet oxygen generation through the FRET.

Scheme 1

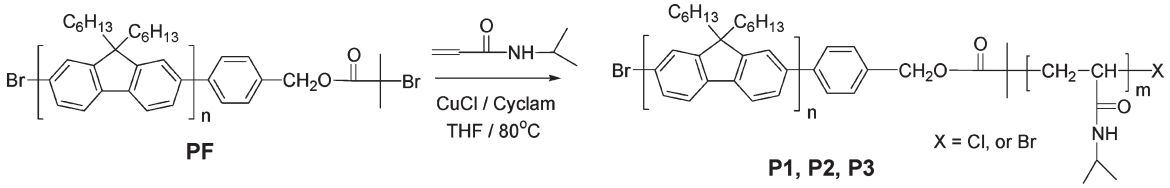

PF: n = 10. $M_{n(GPC)}$ = 2200, M_w/M_n = 1.54, $M_{n\,(NMR)}$ = 3600
P1: n = 10, m = 130. $M_{n(GPC)}$ = 5000, M_w/M_n = 1.83, $M_{n\,(NMR)}$ = 18300
P2: n = 10, m = 310. $M_{n(GPC)}$ = 14400, M_w/M_n = 1.80, $M_{n\,(NMR)}$ = 38600
P3: n = 10, m = 640. $M_{n(GPC)}$ = 31900, M_w/M_n = 2.68, $M_{n\,(NMR)}$ = 75900

liposomes or block copolymers[9] to retain their photoactivities and enable their applications in a biocompatible environment.

Herein, we explore the encapsulation of a water-insoluble porphyrin (tetrakis(mesityl)porphyrin, $H_2(Me_3)TPP$, Figure 1) into the micelles of a new PF-*b*-PNIPAAm. By taking the advantage of the fluorescence property of the PF moiety, we hypothesize that when $H_2(Me_3)TPP$ is physically trapped into the micellar cores, the PF can act as an electron-donating group to transfer its energy to $H_2(Me_3)TPP$ (the acceptor) through fluorescence resonance energy transfer (FRET) process and further increase the singlet oxygen generation from $H_2(Me_3)TPP$ molecules (Figure 1). Along the line of our investigations of the utilization of the block copolymers to fine-tune materials functionality,[10] we will also report the solvent-stimulated emission properties and morphologies of the new series of rod−coil diblock PF-*b*-PNIPAAms.

Experimental Section

Characterizations. ^1H NMR spectra were measured using a Bruker 300 instrument spectrometer operating at 300 MHz. Polymer molecular weights were determined using a Waters 1515 GPC coupled with UV and RI detectors, in reference to a series of polystyrene standards with tetrahydrofuran (THF) as the eluent. UV−vis absorption spectra were measured using a Perkin-Elmer Lambda 9 UV/vis/NIR spectrophotometer. Fluorescence spectra were recorded with an Oriel InstaSpec IV spectrograph that had a charge coupled device (CCD) detector. Fluorescence quantum yields for PF were obtained by comparing the integrated fluorescence spectra of the polymers in solutions to the fluorescence spectrum of quinine sulfate in 1.0 N H_2SO_4 ($\Phi = 0.55$, excitation wavelength of 365 nm)[11] with a correction of refractive index differences. Fluorescence quantum yields for $H_2(Me_3)TPP$ in micelles were obtained by comparing its integrated fluorescence spectrum in toluene ($\Phi = 0.11$, excitation wavelength of 514 nm)[12] with a correction of refractive index differences.

Transmission electron microscopy (TEM) images were obtained using a Philips EM410 microscope operated at 100 kV. TEM samples were prepared by dropping a liquid sample (4 μL) onto a carbon-coated TEM copper grid that dried at room temperature overnight. In order to enhance the contrast of images, the speciments on the TEM grids were stained using the vapor of 0.5 wt % RuO_4 aqueous solution for 2 min. Atomic force microscopy (AFM, NanoScope III, Digital Instrument) equipped with an integrated silicon tip/cantilever with resonance frequency of ~240 kHz in height and phase image models were utilized for the observation of morphologies. Polymer solutions (4 μL) were dropped on a mica sample stage and dried at 4 °C for the morphological observation. The AFM topographies showed no evidence of tip-induced modification during successive scans. Dynamic light scattering (DLS) measurements were performed using a Malvern Nano-ZS instrument equipped with a 4 mW He−Ne laser (633 nm). The solution was filtered through a 0.45 μm Millipore Millex-HN filter to remove dust before DLS measurements.

Materials. 1,4,8,11-Tetramethyl-1,4,8,11-tetraazacyclotetradecane (Me_4Cyclam), *N,N,N′,N″,N″*,-pentamethyldiethylenetriamine (PMDETA), and anhydrous anisole were purchased from Aldrich and used without purification. CuCl (Aldrich) was washed with acetic acid and ether and then dried under vacuum. NIPAAm (Aldrich) was purified by recrystallization twice from hexane. THF and ether were distillated from sodium/benzophenone under nitrogen. $H_2(Me_3)TPP$ was prepared according to a known procedure.[13] Disodium salt of 9,10-anthracenedipropionic acid (ADPA) was purchased from Molecular Probes.

Synthesis. The preparation of the block copolymer is shown in Schemes 1 and 2.

The PF initiator was α-{4-[2-(2-bromo-2-methylpropoyloxy)methyl]phenyl}-ω-bromopoly[2,7-(9,9-dihexylfluorene)]. The PF macroinitiator was prepared according to our previous publication.[10b] $M_{n(GPC)}$=2200, M_w/M_n=1.54. $M_{n(NMR)}$=3600. The degree of polymerization (DP) of PF is 10 determined by ^1H NMR. ^1H NMR (300 MHz, $CDCl_3$): δ = 0.60−0.98 and 1.05−1.31 (s, b, 220H), 1.91 (s, 6H), 1.80−2.26 (m, 40H), 5.22

Scheme 2

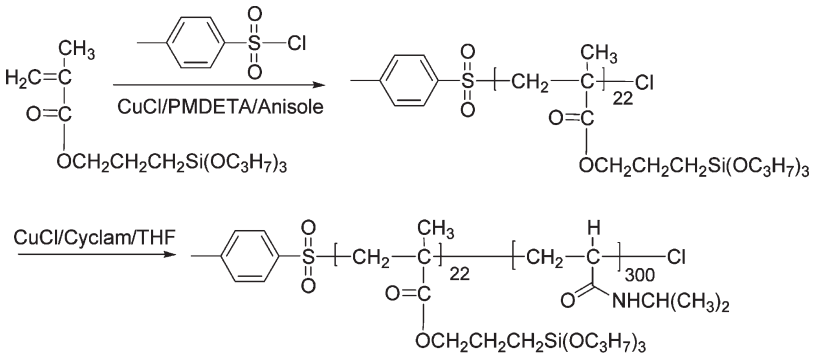

P4, $M_{n(GPC)}$ = 28000, M_w/M_n = 1.21, $M_{n(NMR)}$ = 40500

(s, 2H), 7.34−7.39 (m, 2H), 7.42−7.60 (m, 2H), 7.58−7.92 (m, 60H).

Poly[2,7-(9,9-di-*n*-hexylfluorene)]-*b*-poly(*N*-isopropylacrylamide) (PF-*b*-NIPAAm, **P2**). 20 mg (∼0.0056 mmol) of PF macroinitiator, 2.1 mg of CuCl (0.02 mmol), and 678 mg of NIPAAm monomer (5.68 mmol) were added into a Schlenk tube and then vacuumed for 10 min. Under a nitrogen atmosphere, a solution of 9.8 mg (0.038 mmol) of Me_4Cyclam in 5 mL of THF was added into the Schlenk tube. The mixture was degassed three times and then filled with argon. After stirring at ambient temperature for 30 min, the Schlenk tube was immersed into an oil bath at 80 °C for 16 h. The mixture was then cooled down to room temperature, passed through an Al_2O_3 column to remove the copper complexes, and then precipitated into an excess amount of ether, resulting in 330 mg of **P2** as a white solid in 40% yield. $M_{n(GPC)}$ = 14 400, M_w/M_n = 1.80. ^{1}H NMR (300 MHz, $CDCl_3$): δ = 0.60−0.98 (CH_3) and 1.05−2.41 (br, m, CH and CH_2), 4.0 (br, NCH), 6.0−6.5 (br, NH), 7.3−7.9 (aromatic proton). The DP of the PNIPAAm is calculated to be 310 using eq 1:

$$DP_{PNIPAAm} = (I_{4.0}/1)/(I_{7.3-8.0}/64) \quad (1)$$

where $I_{4.0}$ is the integration of the proton of (NH*CH*$(CH_3)_2$) at 4.0 ppm from the PNIPAAm segment and $I_{7.3-8.0}$ is the integration of the aromatic protons (64H) from the phenyl units. Therefore, $M_{n(NMR)}$ is calculated to be 38 600 using eq 2:

$$M_{n(NMR)} = 3600 + 113 \times DP_{NIPAAm} \quad (2)$$

where DP_{NIPAAm} is 310; 3600 and 113 are the molecular weights of the PF block and NIPAAm monomer, respectively.

Poly[3-(tripropoxysilyl)propyl methacrylate] (PPOPS initiator). 11.4 mg (∼0.06 mmol) of *p*-toluenesulfonyl chloride, 6.0 mg of CuCl (0.06 mmol), and 2.0 g (6 mmol) of the monomer of 3-(tripropoxysilyl)propyl methacrylate[10b] were added into a Schlenk tube and then vacuumed for 10 min. Under a nitrogen atmosphere, a solution of 10.8 mg (0.06 mmol) of PMDETA in 5 mL of anisole was added into the Schlenk tube. The mixture was degassed three times and then filled with argon. After stirring at ambient temperature for 30 min, the Schlenk tube was immersed into an oil bath at 80 °C for 16 h. The mixture was cooled to room temperature, passed through an Al_2O_3 column to remove the copper complexes, and then precipitated into an excess amount of methanol, resulting in 450 mg of poly-[3-(tripropoxysilyl)propyl methacrylate] homopolymer as a white waxy product in 23% yield. $M_{n(GPC)}$ = 10 400, M_w/M_n = 1.06. $M_{n(NMR)}$ = 6600. DP_{PPOPS} = 22.

Poly[3-(tripropoxysilyl)propyl methacrylate]-*block*-poly(*N*-isopropylacrylamide) (**P4**). 100 mg (∼0.015 mmol) of the PPOPS macroinitiator, 3.0 mg of CuCl (0.03 mmol), and 1.0 g (8.9 mmol) of the monomer of NIPAAm were added into a Schlenk tube and then vacuumed for 10 min. Under a nitrogen atmosphere, a solution of 7.8 mg (0.03 mmol) of Me_4Cyclam in 4 mL of THF was added into the Schlenk tube. The mixture was degassed three times and then filled with argon. After stirring at ambient temperature for 30 min, the Schlenk tube was immersed into an oil bath at 80 °C for 16 h. The mixture was cooled to room temperature, passed through an Al_2O_3 column to remove the copper, and then precipitated into an excess amount of ether, resulting in 200 mg of **P4** as a white solid in 20% yield. $M_{n(GPC)}$ = 28 000, M_w/M_n = 1.21. $M_{n(NMR)}$ = 40 500. DP_{NIPAAm} = 300.

Preparation of Polymer Solutions with Nanostructures. *Preparation of Aqueous Solution of PF-b-PNIPAAm.* 4 mg of block copolymer, **P2** or **P3**, was suspended in 4 mL of H_2O. The mixture was then stirred at room temperature for 1 day to obtain a clear solution of the polymer in water (1 mg/mL). The solution was filtered through a 0.45 μm microfilter and diluted to 0.1 mg/mL before use.

Preparation of THF/Toluene (1:10 by Volume) Solution. 1 mL of **P1** or **P2** in THF (concentration: 1.0 mg/mL) was added slowly into 10 mL of toluene, resulting in a clear solution with a concentration of 0.091 mg/mL. The solution was stabilized at room temperature for 2 days before any measurements.

Physical Loading of the $H_2(Me_3)$TPP in PF-b-PNIPAAm Polymeric Micelles. The $H_2(Me_3)$TPP was incorporated into PF-*b*-PNIPAAm polymeric micelles (**P2** was used as an typical example) using the following method, which involved slow injection of a mixture of 100 μL of the block polymer (4 mg/mL in THF) and 100 μL of the $H_2(Me_3)$TPP with various concentrations in THF into 4 mL of distilled water using a syringe, resulting in clear solutions with a consistent concentration of **P2** (0.095 mg/mL) in aqueous solution. The total THF concentration was controlled to be 5 vol % in water. THF was used as cosolvent to increase the loading density of $H_2(Me_3)$TPP into the **P2** micelles. The initial $H_2(Me_3)$TPP loading varied from 0.02 to 2% (w/w, $H_2(Me_3)$TPP/**P2**). The mixture was first stabilized at room temperature for 2 days to incorporate the hydrophobic $H_2(Me_3)$TPP inside the hydrophobic core of the **P2** polymeric micelles. Then, the solutions were filtered through a 0.20 μm microfilter to eliminate excess nonincorporated $H_2(Me_3)$TPP. The amount of $H_2(Me_3)$TPP loaded into the micelles was determined using UV−vis spectra.

Absorbance of porphyrin was measured at 512 nm to avoid the influence by PF, and the absorbance of PF was measured at 365 nm. Their feed concentrations by moles were defined as ($Con_{P2\text{-feed}}$ or $Con_{H2(Me3)TPP\text{-feed}}$). After the **P2**/$H_2(Me_3)$TPP hybrid micelles were prepared, UV−vis spectra were measured. As there are some nonincorporated $H_2(Me_3)$TPP, the solutions were filtered using 0.2 μm filter. After the filtration, UV−vis spectra were measured again. The concentrations of the **P2** ($Con_{P2\text{-determined}}$) and $H_2(Me_3)$TPP ($Con_{H2Me3TPP\text{-determined}}$)

Table 1. Experimental Conditions and Properties of the Polymers

polymer	$[M]_0/[I]_0$[a]	time[e]	$M_{n(GPC)}$[f]	$M_{n(NMR)}$[g]	M_w/M_n[h]	yield (%)[i]	PF (wt %)[j]
PF			2 200	3 600	1.54		100
P1	220[b]	14	5 000	18 300	1.83	23	19.6
P2	1200[b]	16	14 400	38 600	1.80	40	9.4
P3	3000[b]	16	31 900	75 900	2.68	20	4.7
PPOPS	100[c]	16	10 400	6 600	1.06	23	0
P4	590[d]	16	28 000	40 500	1.21	20	0

[a] Feed molar ratio of the monomer $[M]_0$ to initiator $[I]_0$. [b] [PF]:[Cyclam]:[Cu(I)Cl] = 1:2:2. [c] [Toluenesulfonyl chloride]:[PMDETA]:[Cu(I)Cl] = 1:1:1. [d] [PPOPS]:[Cyclam]:[Cu(I)Cl] = 1:2:2. [e] Polymerization time in hours. [f] Number-average molecular weight determined by GPC. [g] Molecular weight determined by ^{1}H NMR. [h] Polydispersity determined by GPC. [i] Yields of the block copolymers from the ATRP process. [j] Weight fraction of the PF in the block copolymers.

were calculated based on the absorbance. The absorbance of PF segments in the micelles before and after filtration had no change as the PF was chemically conjugated with the block copolymer **P2** and assembled in the micellar cores. Absorbance of the $H_2(Me)_3TPP$ decreased depending on the feed amounts, indicating there are some nonincorporated porphyrins. The determined ratios by moles were calculated basing on $Con_{H2Me3TPP\text{-}determined}/Con_{P2\text{-}determined}$. The determined ratios by weights were calculated basing on $(783 \times Con_{H2Me3TPP\text{-}determined})/(38600 \times Con_{P2\text{-}determined})$, where 783 is the molecular weight of $H_2(Me_3)TPP$ and 38600 is the molecular weight of the **P2** determined by ^{1}H NMR.

*Physical Loading of the $H_2(Me_3)TPP$ in **P4** Polymeric Micelles*. The method is the same as that of **P2**.

Results and Discussion

Polymer Synthesis and Characterization. Block copolymers were prepared using atom transfer radical polymerization (ATRP).[14] The polymerizations were carried out at 80 °C in THF with the CuCl/Me_4Cyclam complex as the catalyst system.[15] By controlling the feed ratios of NIPAAm monomer to PF initiator, three block copolymers **P1**, **P2**, and **P3** with different DPs of PNIPAAm were obtained. Detailed experimental conditions and physical data of the three block copolymers are given in Table 1. GPC curves of the PF macroinitiator and its block copolymers are depicted in Figure 2. The GPC profiles of the block copolymers shift to high molecular weight regions with an increase in feed ratios. For all of the block copolymers, no residual macroinitiators remained, implying that all of the macroinitiators worked well to initiate the polymerization. However, the block copolymers exhibited wide polydispersities and yields were low (Table 1). Two possibilities that could contribute to the high polydispersity include (i) polydispersity of the PF initiator is 1.54, which is not low since the PF was prepared through a Suzuki coupling, and (ii) the CuCl/Cyclam catalyst system for the polymerization of acrylamide or methacrylamide monomers is not a well-controlled catalyst system due to a slow deactivation rate of the catalytic system for the acrylamide or methacrylamide monomers.[16] The low yields are most likely related to (i) low conversions of the polymerizations in our systems and (ii) a loss during our work-up process to purify the polymers. For the synthesis of **P2**, a conversion of 55% was determined by ^{1}H NMR, and the purified yield was 40%. The purified polymers were analyzed using ^{1}H NMR (Figure 3A) to determine the weight percentage of the PF in its PF-*b*-PNIPAAm. Data are given in Table 1. For a comparison of the singlet oxygen generation efficiency of $H_2(Me_3)TPP$ in micelles, **P4** was prepared as a non-PF-containing block copolymer.

Nanostructures of the PF-*b*-PNIPAAms. In order to investigate solvents stimulated functionality and nanostructures, water and a mixed organic solvent of THF/toluene (1:10 by volume) were chosen. Water is a good solvent for the PNIPAAm block at room temperature but a nonsolvent for the PF segments. The mixture of THF and toluene is a good solvent for PF whereas a poor solvent for the PNIPAAm chain. **P1** is soluble in THF/toluene mixture but insoluble in water. **P3** is readily soluble in water while insoluble in the THF/toluene mixture. **P2** has a good solubility in either water or THF/toluene. These variations of solubility (Table 2) showed a significant influence of the polymer structures on their solubility, which should be attributed to their different abilities of forming nanostructures due to the various length ratios of the PF to PNIPAAm segment.

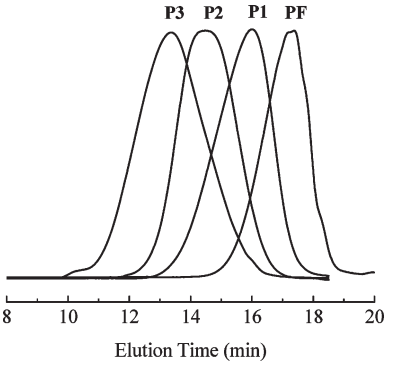

Figure 2. GPC profiles of the macroinitiator PF and its three diblock copolymers of **P1**, **P2**, and **P3**. For PF, $M_{n(GPC)} = 2200$, $M_w/M_n = 1.54$, $M_{n(NMR)} = 3600$. For **P1**, $M_{n(GPC)} = 5000$, $M_w/M_n = 1.83$, $M_{n(NMR)} = 18\,300$. For **P2**, $M_{n(GPC)} = 14\,400$, $M_w/M_n = 1.80$, $M_{n(NMR)} = 38\,600$. For **P3**, $M_{n(GPC)} = 31\,900$, $M_w/M_n = 2.68$, $M_{n(NMR)} = 75\,900$.

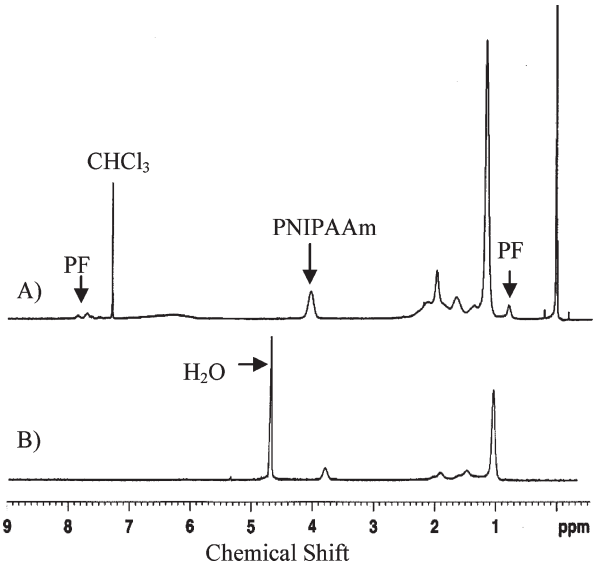

Figure 3. ^{1}H NMR spectra of the block copolymer **P2** in $CDCl_3$ (A) and D_2O (B).

Table 2. Physical Properties and Nanostructures of P1, P2, and P3

	solvent	solubility	λ_{max}[a] (nm)	λ_{max}[b] (nm)	Φ[c]	nanostructures DLS[d]	AFM[e]	TEM[f]
P1	water	insoluble						
P1	THF/toluene	soluble	370	421	0.83	g	90 ± 40	110 ± 70
P2	water	soluble	365	447	0.26	44 (0.23);	40 ± 30	18 ± 10
P2	THF/toluene	soluble	370	421	0.80	161 (0.15)	170 ± 90	150 ± 70
P2	THF	soluble	370	421	0.84			
P3	water	soluble	365	447	0.28	62 (0.19);	70 ± 30	25 ± 10
P3	THF/toluene	insoluble						

[a] The absorbance λ_{max} determined from UV−vis spectra. [b] The emission λ_{max} determined from fluorescence spectra excited at 365 nm. [c] Quantum yield. [d] Particle size in solution determined from dynamic light scattering. The number in parentheses is the polydispersity. [e] Observed from AFM on mica surface at the dry state. [f] Observed under TEM at the dry state. [g] No reliable data were obtained due to its very weak signal.

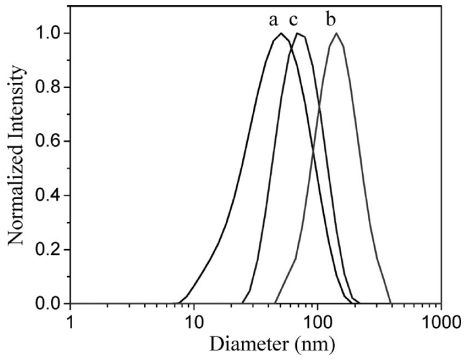

Figure 4. DLS profiles of **P2** in water (curve a), **P2** in THF/toluene (curve b), and **P3** in water (curve c).

Although PF itself is completely insoluble in water, the block copolymer **P2** has a good solubility (up to 10 mg/mL) in water. This property should be attributed to the fact that the block copolymer forms nanostructured aggregates (micelles) with the hydrophilic PNIPAAm block as the corona and the hydrophobic PF block as the core. This is supported by the ^{1}H NMR spectrum in D_2O, as illustrated in Figure 3. It can be seen that all of the peaks assigned to PF disappear completely in D_2O, indicating the formation of aggregates with PF as the core. The DLS result gives further confirmation of the nanostructures. **P2** in the 0.1 mg/mL aqueous solution exhibits an average hydrodynamic diameter of 44 nm (Table 2 and Figure 4) at 25 °C. TEM was used to characterize the nanostructures in the solid state. However, particles with an average diameter of only 18 nm (Table 2 and Figure 5C) were observed, which is much smaller than that found from DLS. Aromatic PF segment is stained easier than PNIPAAm chain, which may result in the observation of the micellar cores formed by the PF chains under TEM. The observation of only the cores of micelles by TEM was reported by other scientists.[17] Therefore, AFM images were used to characterize the micelles dried from the water solution (Table 2 and Figure 5D). The dried sample for AFM imaging was prepared at 4 °C because it was found that drying the aqueous solution at room temperature on the mica surface resulted in a continuous film and was therefore difficult for the observation of an individual micelle. When 4 μL of the aqueous solution (0.1 mg/mL of polymer in water) was dried at 4 °C (24 h) on a mica surface, the micelles dispersed well as individual particles ranging from 20 to 65 nm with an average diameter of 40 nm (calculated using 30 individual particles in area 1 with a 1 μm × 1 μm area in Figure 5D) were observed. More interestingly, cylindrical micelles with an average diameter of 50 nm and a length of about 2 μm were observed. Two loops around the cylindrical micelles (indicated by arrows) with an average diameter of 20 nm were also seen. The nonuniform sizes of micelles are

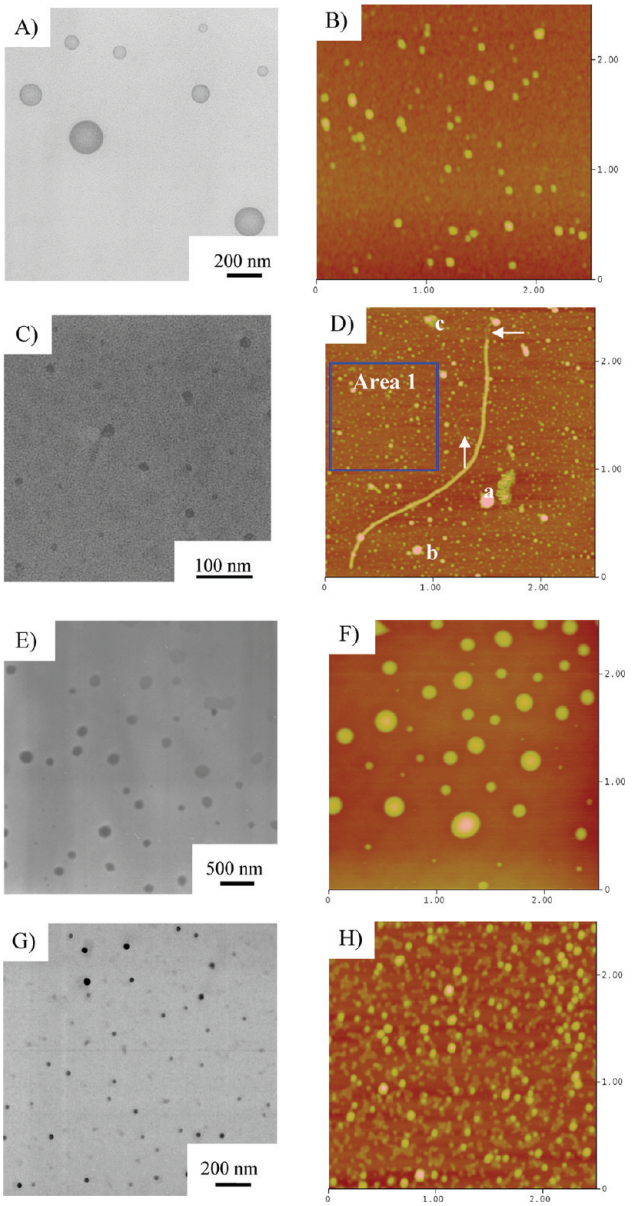

Figure 5. Morphologies of the **P1** dried from THF/toluene (A and B), **P2** dried from water (C and D), **P2** dried from THF/toluene (E and F), and **P3** dried from water (G and H). A, C, E, and G are TEM images; B, D, F, and H are AFM height image (2.5 μm × 2.5 μm). Large aggregates labeled as a, b, and c in (D) are probably due to a few micelles aggregated together during the drying process.

possibly due to the large polydispersity of the block copolymer (M_w/M_n = 1.80). The evaporation process may also possibly affect the morphologies. In general, the average

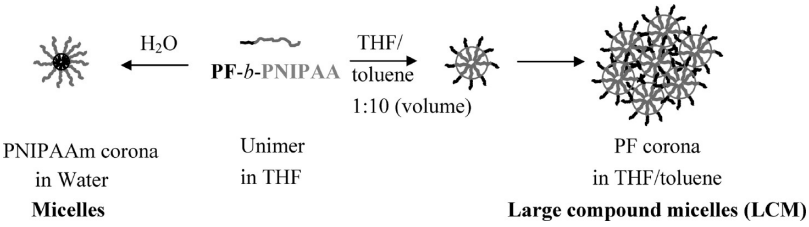

Figure 6. A possible mechanism of the formation of micelles in water and invert LCM in THF/toluene. The chain entanglement pathway (1) as described in text was used to show the possible LCM formation process.

diameter (40 nm) of the dried micelles is in good accordance with that from DLS. In the case of the large aggregates, such as the particles of a, b, and c, it is possible that a few micelles aggregated together during the drying process.

Although the PNIPAAm itself is insoluble in THF/toluene, the block copolymer **P2** exhibits a good solubility up to 0.32 mg/mL in the mixed solvent. In this case, the block copolymer tends to form inverse aggregates with the PF as the corona, resulting in the good solubility of the block copolymer in the mixed organic solvents. Large aggregates with an average diameter of 161 nm (Table 2 and Figure 4, DLS), 150 ± 70 nm (Table 2 and Figure 5E, TEM image), and 170 ± 90 nm (Table 2 and Figure 5F, AFM image) were observed either in solution or in dried states. Such large aggregates are more like the large compound micelles (LCMs, Figure 6).[18] Two possible pathways[18b] can be used to explain the formation of the LCMs: (1) on addition of toluene, the insoluble PNIPAAm aggregated to create a continuous phase with the islands of corona-forming blocks (PFs) nested throughout and surrounded by a coronal shell at the core−solvent interface; (2) simple spheres formed, but corona-chain (PF) flocculation or interpenetration occurred and thus the continuous phase had coronal blocks (PF) with pockets of insoluble blocks (PNIPAAm).

The dried **P1** on mica from THF/toluene also shows the inverse micelles with PF as the corona and PNIPAAm as the core. The average diameters of the inverse micelles are 110 ± 70 nm (Figure 5A, TEM image) and 90 ± 40 (Figure 5B, AFM image). **P3** in water exhibits the micellar structures with an average diameter of 62 nm measured by DLS (Table 2 and Figure 4). The observed diameter, 25 ± 10 nm, of dried **P3** micelles measured with TEM (Figure 5G) is much smaller than measured by AFM, 70 ± 30 nm (Figure 5H). This phenomenon was observed in **P2** and explained before.

Photophysical Properties of PF-*b*-PNIPAAm. Photophysical properties (UV−vis and fluorescence emission spectra) of the block copolymers were studied in water and the mixed organic solvent of THF/toluene at room temperature. Similar photophysical properties were observed between **P2** and **P3** in water (Table 2). The similar tendency was also observed between **P1** and **P2** in THF/toluene (Table 2). For comparison, the photophysical properties of **P2** in THF, a good solvent for both the PF and PNIPAAm chains, were also measured. The typical photophysical properties of **P2** are illustrated in Figure 7A. The shapes of absorption and emission spectra of **P2** in THF and THF/toluene have no obvious difference. However, in water, the absorption spectrum presents a peak at 365 nm with a 5 nm blue shift compared with that in THF (peak at 370 nm). In addition, the fluorescence spectrum in water is quite different from that in THF or THF/toluene mixture. An additional featureless emission band appears at a longer wavelength (500−600 nm), and the third vibrational band at ~470 nm becomes much stronger. Meanwhile, the relative intensities

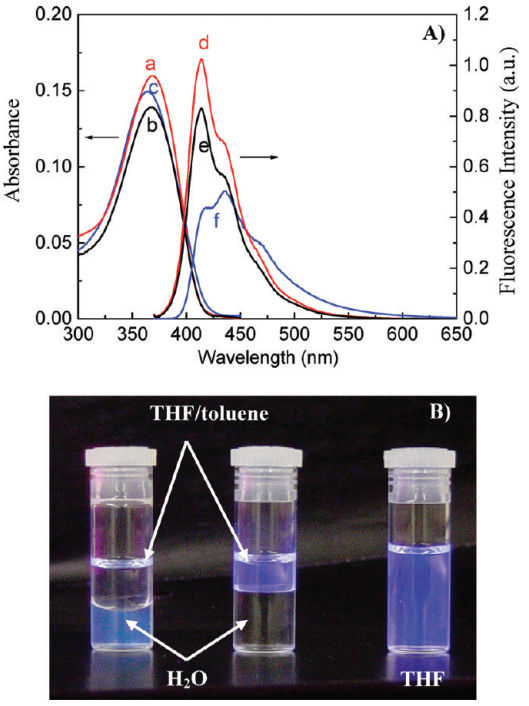

Figure 7. UV−vis and fluorescence spectra (A) of **P2** and its fluorescence images (B). Curve a is the UV−vis spectrum in THF; curve b is the UV−vis spectrum in THF/toluene; curve c is the UV−vis spectrum in H_2O; curve d is the fluorescence emission in THF; curve e is the fluorescence emission in THF/toluene; curve f is the fluorescence emission in H_2O. The fluorescence emissions were excited at 365 nm. The left image in (B) shows the selective solubility of **P2** in H_2O with weak sky-blue emission; the middle image in (B) shows the selective solubility of **P2** in THF/toluene with strong blue emission; the right image in (B) shows the strong blue emission in THF.

of the first (421 nm) and the second (447 nm) vibrational bands in the emission spectrum are reduced significantly as compared to those in THF.

The different functionality should be attributed to their different nanostructures stimulated by the solvents. In water, the polymers form micelles with PF as the core, resulting in much stronger aggregation of the PF chains due to enhanced $\pi-\pi$ interactions or hydrophobic−hydrophobic interactions of the PF segments in the micellar cores. Because of the aggregation, PF shows a significant amount of excimer emission.[19a] Although the appearance of such excimer emission is very common for PF polymers upon heating,[19] the result of **P2** suggests that the formation of excimers may be facilitated in PF aggregates with tight intermolecular packing only through the micelle formation. Because of the strong aggregations of PFs in the micellar core, a blue-shifted effect was observed from the absorption of **P2** in water. The blue shift indicates H-aggregations[20] of the PF moieties, resulting in a much easier formation of the excimers.[1i,20] Because of

the appearance of excimers, the fluorescence quantum efficiency of the PF segments decreased to 0.26 in pure water from 0.84 in THF, resulting in the sky-blue emission with weak fluorescence intensity. In contrast, the block copolymers in the mixed THF/toluene solvent formed the inverted micelles with PF as the corona. The PF segments did not show obvious aggregations exhibiting a quantum yield of 0.80 because they were well dispersed and dissolved in THF/toluene, resulting in similar photophysical properties in the THF/toluene mixture as those in THF.

Because of the different nanostructures as discussed above, the polymer **P2** can be dissolved selectively in water or THF/toluene mixture. When the micelles were prepared from water, the corona was PNIPAAm, rendering the polymer soluble in water but insoluble in THF/toluene (left image in Figure 7B). When the micelles were prepared from THF/toluene, the corona was PF, which makes the polymer insoluble in water (middle image in Figure 7B). Because of the fluorescent character of the PF, the above hypothesis was visualized directly using the fluorescence images shown in Figure 7B. For comparison, the fluorescence image of **P2** in THF was also given in Figure 7C. Recall the different nanostructures also affected the fluorescence properties; weak sky-blue emission was observed in water (left image in Figure 7B), and strong blue-emission was observed in THF/toluene (middle image in Figure 7B) with a similar brightness to that in THF (right image in Figure 7B). Therefore, the photophysical property and solubility of the new amphiphilic functional block copolymer were successfully controlled through the solvent stimuli.

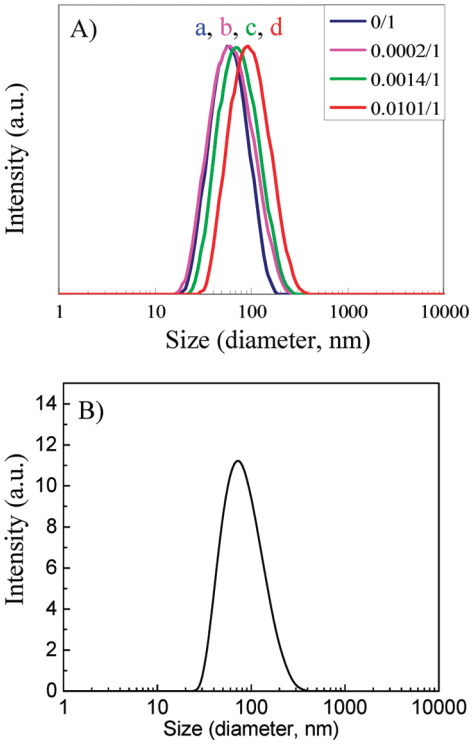

Figure 8. (A) Size distributions of the micelles of $H_2(Me_3)TPP$/**P2** solutions with different $H_2(Me_3)TPP$ loading ratios (by weight). For all the measurements, the **P2** has the same concentration of 0.095 mg/mL. a, b, c, and d correspond to the weight ratios of $H_2(Me_3)TPP$/**P2** of 0, 0.0002, 0.0014, and 0.01. (B) Size distribution of the micelles of $H_2(Me_3)TPP$/**P4** solution with the $H_2(Me_3)TPP$/**P4** load ratios (by weight) of 0.0014.

Encapsulation of $H_2(Me_3)TPP$ into P2's Micelles: FRET Investigation. For this study, the micelles were generated in aqueous solution containing 5 vol % THF with a consistent **P2** concentration of 0.095 mg/mL (2.6×10^{-6} mol/L) at room temperature. In this experimental condition, the quantum yield of PF in the micelles is 0.34. The hydrophobic $H_2(Me_3)TPP$ does not fluoresce in aqueous solution, but it starts to fluoresce with emission bands at 650 and 724 nm and with a fluorescence quantum yield of 0.065[21] once it is encapsulated inside micelles. Average diameters of micelles of the $H_2(Me_3)TPP$/**P2** complexes were in the range of 50−87 nm (Figure 8A and Table 3), increasing directly with the concentration of the encapsulated $H_2(Me_3)TPP$, which were determined by DLS in solution and further observed by AFM in a dried state (Figure 9).

Figure 10A gives the absorbance and emission spectra of PF and $H_2(Me_3)TPP$. Curves a and b are the absorbance of PF and $H_2(Me_3)TPP$, respectively. Curve c is a 10-fold magnification of curve b to enlarge the Q-bands of the porphyrin. Curves d and e are the emission spectra of PF and $H_2(Me_3)TPP$, respectively. The fluorescence band of PF (curve d) significantly overlaps with the absorption of $H_2(Me_3)TPP$ (curves b and c). This spectral overlap indicates efficient energy transfer may occur from PF to $H_2(Me_3)TPP$ at suitable conditions.

In the micelle-containing aqueous solution, with an increased $H_2(Me_3)TPP$ concentration, fluorescence intensity of PF decreases (Figure 10B). Depending on the concentration of $H_2(Me_3)TPP$, a calculated energy transfer efficiency[22] of 30−98% was observed (inset in Figure 10B and Table 3). Furthermore, excitation of the complexes with the $H_2(Me_3)TPP$ loadings of 0.02 and 0.14 wt % (runs 2 and 3 in Table 3) at 380 nm (the excitation of the donor of PF) ($F_{ex380nm}$) results in ~10.2- and 1.5-fold increase in the area of emission from $H_2(Me_3)TPP$, compared to the direct excitation of $H_2(Me_3)TPP$ at 418 nm ($F_{ex418nm}$). One example using the $H_2(Me_3)TPP$ loading ratio of 0.14 wt % is given in Figure 10C. Curve h was excited at 380 nm, and curve j was excited at 418 nm. This phenomenon is called the "antenna effect". The concentration-dependent "antenna effect" calculated using $F_{ex380nm}/F_{ex418nm}$ is given in the inset of Figure 10C. This "antenna effect" is the result of the larger extinction coefficients of the complexes at 380 nm than at

Table 3. Properties of $H_2(Me_3)TPP$ in Micellar Aqueous Solutions

	feed ratio[c]		determined ratio[d]				average diameters of the micelles	
runs	by weight	by mole	by weight	by mole	ET (%)[e]	AM[f]	DLS[g]	AFM[h]
1[a]	0	0	0	0	0	0	50 (0.22)	59 ± 12
2[a]	0.0002	0.01	0.000 20	0.01	30	22	54 (0.23)	i
3[a]	0.002	0.1	0.0014	0.067	92	8	66 (0.22)	61 ± 30
4[a]	0.02	1	0.0101	0.5	98	7	87 (0.20)	i
5[b]	0.0014	0.073	0.0014				70 (0.20)	i

[a] Runs 1−4 are for $H_2(Me_3)TPP$ in **P2** micelles. [b] Run 5 is an example of $H_2(Me_3)TPP$ in **P4** micelles. [c] Feed ratios of $H_2(Me_3)TPP$ to **P2** or **P4**. [d] The relative ratios of $H_2(Me_3)TPP$ to **P2** were determined by UV−vis spectra (see Experimental Section for details). [e] Energy transfer efficiency. [f] Amplification effect. [g] Determined by dynamic light scattering in solution at 25 °C. The data in parentheses are the polydispersities. [h] Observed by atomic force microscopy. [i] Not measured.

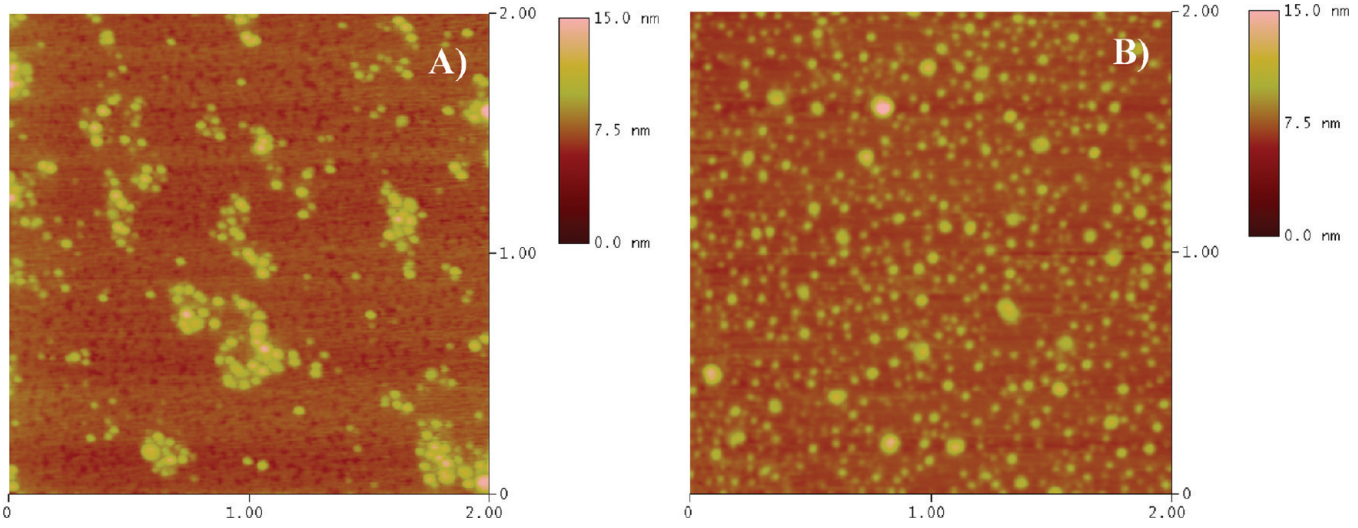

Figure 9. AFM height images (2 μm × 2 μm) of the dried **P2** (A) and the dried $H_2(Me_3)TPP$/**P2** (B, 0.0014:1 by weight) from 5% THF aqueous solutions.

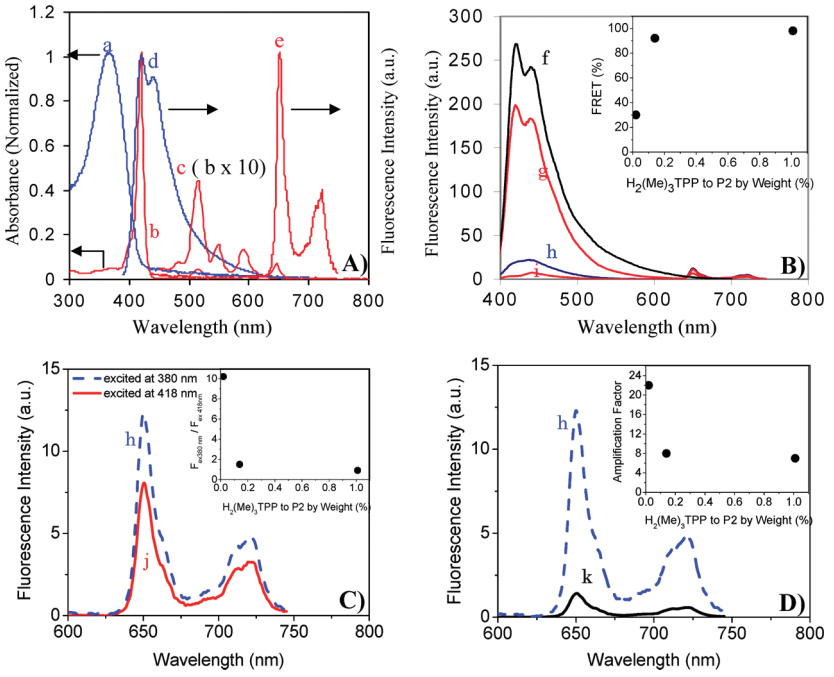

Figure 10. UV−vis and steady fluorescence spectra of the donor (PF) and acceptor ($H_2(Me_3)TPP$) (A), emission spectra of the **PF** with different amounts of $H_2(Me_3)TPP$ in **P2** (curves f−i in B), typical "antenna effect" of $H_2(Me_3)TPP$ in **P2** (curves h and j in C), and typical amplification effect $H_2(Me_3)TPP$ by **P2** (curve h in D) referred to the emission intensity of $H_2(Me_3)TPP$ in **P4** (curve k). a is the UV−vis spectrum of **P2**; b is the UV−vis spectrum of $H_2(Me_3)TPP$ loaded into **P4**; c is the magnified Q-band from $H_2(Me_3)TPP$; d is the emission of PF excited at 380 nm; e is the emission of $H_2(Me_3)TPP$ excited at 418 nm; f, g, h, and i are the emission spectra of $H_2(Me_3)TPP$/**P2** with the loading ratios of 0, 0.02, 0.14, 1.01 wt % excited at 380 nm; j is the emission of $H_2(Me_3)TPP$/**P2** with the loading ratio of 0.14 wt % excited at 418 nm, and k is the emission of $H_2(Me_3)TPP$/**P4** with the loading ratio of 0.14 wt % excited at 380 nm. Integrated fluorescence intensities of h and j are for the antenna effect calculation. Integrated fluorescence intensities of h and k are for the amplification calculation.

418 nm (see Supporting Information, S-Figure 2, for their UV−vis spectra). Excitation of the complex in the aqueous solution with the $H_2(Me_3)TPP$ loading of 1.01 wt % (run 4 in Table 1) at 380 nm shows a slight (~10%) decrease in the area of emission from $H_2(Me_3)TPP$, compared to its direct excitation at 418 nm. But this phenomenon is due to the higher molar absorptivity of the complex at 418 nm than at 380 nm and is not evidence of inefficient energy transfer. It should be noted that no antenna effect or significant quenching of the PF donor emission was observed in the mixtures of $H_2(Me_3)$-TPP and **P2** in THF, where there is no micellar structures (see Supporting Information, S-Figure 4). Therefore, the above studies indicated $H_2(Me_3)TPP$ interacted well with PF inside the micellar cores via the noncovalent bonding and effective FRET[23] occurred from PF to $H_2(Me_3)TPP$.

In order to study the amplification effect, a block copolymer of poly[3-(tripropoxysilyl)propyl methacrylate]-*block*-poly(*N*-isopropylacrylamide) (**P4**, Scheme 2), without the PF donor, was used as a counterpart to encapsulate the dye. Referring to the fluorescence intensities of $H_2(Me_3)TPP$ in **P4** micelles ($F_{H_2(Me_3)TPP/P4}$) excited at 380 nm, the amplification factors (AM, see eq 3 for the definition) of $H_2(Me_3)TPP$ by PF ($F_{H_2(Me_3)TPP/PF}$) were calculated to be 22, 8, and 7, respectively (Table 3). A typical example of the amplification

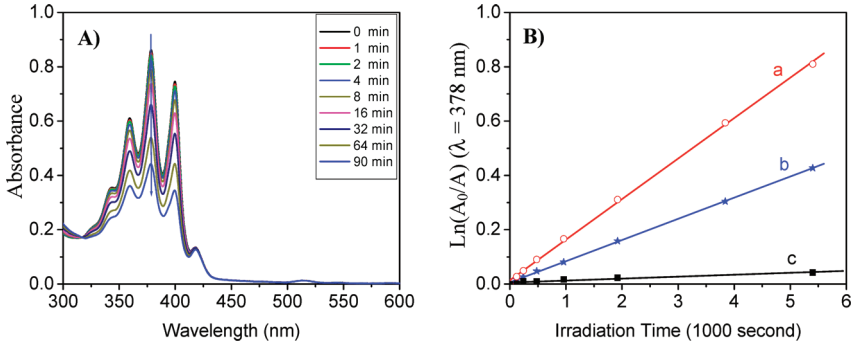

Figure 11. Typical photochemical process of $H_2(Me_3)TPP$/**P2**/ADPA (A) and the first-order plots for the photooxidation of ADPA (B) in $H_2(Me_3)TPP$/**P2**/ADPA (curve a), $H_2(Me_3)TPP$/**P4**/ADPA (curve b), and **P2**/ADPA (curve c). A_0 is the absorbance at 378 nm before irradiation. A is the absorbance after irradiation. The weight ratio of $H_2(Me_3)TPP$ to block copolymer is 0.14 wt %. Concentration for block copolymers is 0.095 mg/mL. Concentration for ADPA is 2×10^{-5} M.

effect using $H_2(Me_3)TPP$ loading ratio of 0.14 wt % was given in curve h (emission spectrum of $H_2(Me_3)TPP$/**P2**) and curve k (emission spectrum of $H_2(Me_3)TPP$/**P4**) in Figure 10D. The concentration-dependent amplification effect was also given in the inset of Figure 10D.

$$\mathrm{AM} = F_{H_2(Me_3)TPP/PF}/F_{H_2(Me_3)TPP/\mathbf{P4}} \quad (1)$$

The above photophysical study indicated that the PF and $H_2(Me_3)TPP$ could be forced to be closer than 10 nm in the micellar cores, which is the requirement for the occurrence of FRET.[23] These results showed that PF could be utilized as a donor to efficiently generate porphyrin excited states and the FRET could be observed between the noncovalently bonded PF and $H_2(Me_3)TPP$ inside the micelles.

Enhancement of the Singlet Oxygen Generation of $H_2(Me_3)TPP$ by FRET. The ability to generate $^1O_2$ was evaluated by a chemical method, using the disodium salt of 9,10-anthracenedipropionic acid[24] (ADPA, Molecular Probes) as a water-soluble $^1O_2$ sensor. The $^1O_2$ is quenched by ADPA, resulting in the bleach of ADPA to its corresponding endoperoxide. The reaction was monitored spectrophotometrically by recording the decrease in optical density at 378 nm from the ADPA absorption. Micellar solutions were irradiated using a 365 nm (light intensity: 0.84 mW/cm^2) monochromatic light. For comparison, three different oxygen-saturated aqueous solutions (**P2**/ADPA, $H_2(Me_3)TPP$/**P4**/ADPA, and $H_2(Me_3)TPP$/**P2**/ADPA) with the same ADPA and/or $H_2(Me_3)TPP$ concentrations were studied. The mixtures were prepared by addition of ADPA to the aqueous micellar solutions of **P2** (run 1 in Table 3), $H_2(Me_3)TPP$/**P4** (run 5 in Table 3), and $H_2(Me_3)TPP$/**P2** (run 3 in Table 3). Here, deuterium oxide (D_2O) was used as a solvent instead of H_2O because the lifetime of singlet oxygen in D_2O (~55−68 ms) is much longer than that in H_2O (~3−4 ms).[25] The solution without $H_2(Me_3)TPP$ produced nearly no change in the absorption of ADPA with increased irradiation time, indicating that the bleaching of ADPA as a function of the time by the irradiating light is negligible. On the contrary, obvious time-dependent decrease in the ADPA absorbance of the mixtures containing $H_2(Me_3)TPP$ was observed (Figure 11A), indicating that singlet oxygen was generated by $H_2(Me_3)TPP$ and could escape from the micelles to react with ADPA. Studies have shown that 50% of the produced singlet oxygen could diffuse ~80 nm before quenched and less than 0.1% could travel 250 nm in aqueous solutions.[25] Values of the observed rate constants (k^{ADPA}, the slope of $\ln(A_0/A)$ at 378 nm against irradiation time; Figure 11B) of $H_2(Me_3)TPP$/**P4**/ADPA (curve b) and $H_2(Me_3)TPP$/**P2**/ADPA (curve a) are $(0.91 \pm 0.2) \times 10^{-4}$ and $(1.81 \pm 0.3) \times 10^{-4}$ s^{-1}, respectively. The bleaching velocity of the non-PF system is half that of the PF-containing system, confirming that the energy transfer from PF to $H_2(Me_3)TPP$ contributes significantly (with an efficiency factor of 2) to the singlet oxygen generation. During the time of the preparation of this manuscript, scientists reported that the PF could exhibit large two-photon absorbing cross sections under near-infrared light excitation.[26] A further work can be the utilization of the near-infrared light as the light excitation source. As compared with the UV−vis light source, the near-infrared light can penetrate much deeper in tissue and reduce photodamage for tissues, which may address the application of the rod−coil block copolymers in the near-infrared light excitable photodynamic therapy.

Conclusions

New amphiphilic polyfluorene-*block*-poly(*N*-isopropylacrylamide) diblock copolymers containing consistent PF segments but different lengths of PNIPAAms were synthesized and investigated. The degree of polymerization of PNIPAAm affects the aggregations of the block copolymers in water and THF/toluene (1:10 by volume), resulting in different solubility and functionality of the block copolymers. One typical block copolymer **P2** with suitable lengths of the PF and PNIPAAm chains can be selectively dissolved in water and the THF/toluene mixture due to the formation of inverted micelles. These micellar nanostructures contribute to their different photophysical properties. In addition, one PF-*b*-PNIPAAm (**P2**) has been utilized as a nanocarrier to incorporate hydrophobic porphyrin, $H_2(Me_3)TPP$ within its micelles, enabling an application of the water-insoluble porphyrin into aqueous solution. Efficient FRET, up to 98% from PF to $H_2(Me_3)TPP$, was observed in the micellar solution. It was shown FRET made a great contribution to the generation of singlet oxygen from the photosensitizer ($H_2(Me_3)TPP$). This is the first time that energy-transfer process of a water-insoluble porphyrin has been explored in an aqueous solution using both the functionality and nanostructures of functional rod−coil diblock copolymers. Therefore, not only the nanostructures and functionalities through the environmental stimuli were successfully controlled using the new amphiphilic functional rod−coil diblock copolymers, but also the micelles were applied to encapsulate a porphyrin to enhance the porphyrin's singlet oxygen generation efficiency through FRET from PF to porphyrin.

Acknowledgment. The authors thank Ms. Patricia Golas and Prof. Shuiqin Zhou at Department of Chemistry, City University of New York, and Prof. Miqin Zhang and Dr. Narayan Bhattarai at the University of Washington for the assistance with the DLS measurements.

Supporting Information Available: Absorbance and emission spectra of $H_2(Me_3)TPP$ in micelles and THF with or without FRET, the choice of experimental conditions, discussion of the quantum yield of the porphyrin, and the stability statement of the PPOPS. This material is available free of charge via the Internet at http://pubs.acs.org.

References and Notes

(1) (a) Jenekhe, S. A.; Chen, X. L. *Science* **1998**, *279*, 1903. (b) Hempenius, M. A.; Langeveld-Voss, B. M. W.; van Haare, J. A. E. H.; Janssen, R. A. J.; Sheiko, S. S.; Spatz, J. P.; Moller, M.; Meijer, E. W. *J. Am. Chem. Soc.* **1998**, *120*, 2798. (c) Liu, J. S.; Sheina, E.; Kowalewski, T.; McCullough, R. D. *Angew. Chem., Int. Ed.* **2002**, *41*, 329. (d) Tsolakis, P. K.; Kallitsis, J. K. *Chem.—Eur. J.* **2003**, *9*, 936. (e) Boer, B.; Stalmach, U.; Nijland, H.; Hadziioannou, G. *Adv. Mater.* **2000**, *12*, 1581. (f) Stalmach, U.; Boer, B.; Videlot, C.; van Hutten, P. F.; Hadziioannou, G. *J. Am. Chem. Soc.* **2000**, *122*, 5464. (g) Wang, H.; Wang, H.; Urban, V. S.; Littrell, K. C.; Thiyagarajan, P.; Yu, L. P. *J. Am. Chem. Soc.* **2000**, *122*, 6855. (h) Tew, G. N.; Pralle, M. U.; Stupp, S. I. *J. Am. Chem. Soc.* **1999**, *121*, 9852. (i) Lu, S.; Fan, Q. L.; Chua, S. J.; Huang, W. *Macromolecules* **2003**, *36*, 304. (j) Lu, S.; Fan, Q. L.; Liu, S. Y.; Chua, S. J.; Huang, W. *Macromolecules* **2002**, *35*, 9875. (k) Kong, X.; Jenekhe, S. A. *Macromolecules* **2004**, *37*, 8180. (l) Lu, S.; Liu, T. X.; Ke, L.; Ma, D. G.; Chua, S.-J.; Huang, W. *Macromolecules* **2005**, *38*, 8494.

(2) (a) Pei, Q.; Yang, Y. *J. Am. Chem. Soc.* **1996**, *118*, 7416. (b) Ranger, M.; Leclerc, M. *Macromolecules* **1999**, *32*, 3306. (c) Ding, J.; Day, M.; Robertson, G.; Roovers, J. *Macromolecules* **2002**, *35*, 3474. (d) Zhan, X.; Liu, Y.; Wu, X.; Wang, S.; Zhu, D. *Macromolecules* **2002**, *35*, 2529. (e) Yu, W. L.; Pei, J.; Huang, W.; Heeger, A. J. *Adv. Mater.* **2000**, *12*, 828. (f) Zeng, G.; Yu, W. L.; Chua, S. J.; Huang, W. *Macromolecules* **2002**, *35*, 6907. (g) Huang, F.; Hou, L.; Wu, H.; Wang, X. H.; Shen, H. L.; Cao, W.; Yang, W.; Cao, Y. *J. Am. Chem. Soc.* **2004**, *126*, 9845.

(3) (a) Gaylord, B. S.; Heeger, A. J.; Bazan, G. C. *J. Am. Chem. Soc.* **2003**, *125*, 896. (b) Fan, Ch. H.; Wang, S.; Hong, J. W.; Bazan, G. C.; Plaxco, K. W.; Heeger, A. J. *Proc. Natl. Aacd. Sci. U.S.A.* **2003**, *100*, 6297.

(4) (a) Marsitzky, D.; Klapper, M.; Müllen, K. *Macromolecules* **1999**, *32*, 8685. (b) Scherf, U.; List, E. J. W. *Adv. Mater.* **2002**, *14*, 477. (c) Schmitt, C.; Nothofer, H.-G.; Falcou, A.; Scherf, U. *Macromol. Rapid Commun.* **2001**, *22*, 624. (d) Lin, C.-H.; Tung, Y.-C.; Ruokolainen, J.; Mezzenga, R.; Chen, W.-C. *Macromolecules* **2008**, *41*, 8759. (e) Kuo, C.-C.; Tung, Y.-C.; Lin, C.-H.; Chen, W.-C. *Macromol. Rapid Commun.* **2008**, *29*, 1711.

(5) (a) Xiao, X.; Fu, Y. Q.; Zhou, J.-J.; Bo, Z. S.; Li, L.; Chan, C. M. *Macromol. Rapid Commun.* **2007**, *28*, 1003. (b) Ma, J.; Qiang, L.; Zheng, Z.; Wang, Y.; Zhang, Z.; Huang, W. *J. Appl. Polym. Sci.* **2008**, *110*, 18.

(6) Heskins, M.; Guillet, J. E. *J. Macromlol. Sci., Part A2* **1968**, 1441.

(7) (a) Pandey, R. K.; Zheng, G. In *The Porphyrin Handbook*; Kadish, K. M., Smith, K. M., Guilard, R., Eds.; Academic Press: Boston, 2000; Vol. *6*, Chapter 43, p 157. (b) Macdonald, I. J.; Dougherty, T. J. *J. Porphyrins Phthalocyanines* **2001**, *5*, 105. (c) Juzeniene, A.; Peng, Q.; Moan *J. Photochem. Photobiol. Sci.* **2007**, *6*, 1234. (d) Calzavara-Pinton, P. G.; Venturini, M.; Sala, R. *J. Eur. Acad. Dermatol. Venereol.* **2007**, *21*, 439.

(8) (a) Allen, C. M.; Sharman, W. M.; Van Lier, J. E. *J. Porphyrin Phthalocyanines* **2001**, *5*, 161. (b) Hone, D. C.; Walker, P. I.; Evans-Growing, R.; FitzGerald, S.; Beeby, A.; Chambrier, I.; Cook, M. J.; Russell, D. A. *Langmuir* **2002**, *18*, 2985.

(9) (a) van Nostrum, C. F. *Adv. Drug Delivery Rev.* **2004**, *56*, 9. (b) Jang, W.-D.; Nishiyama, N.; Zhang, G.-D.; Harada, A.; Jiang, D.-L.; Kawauchi, S.; Morimoto, Y.; Kikuchi, M.; Koyama, H.; Aida, T.; Kataoka, K. *Angew. Chem., Int. Ed.* **2005**, *44*, 419. (c) Konan, Y. N.; Gurny, R.; Allemann, E. *Photochem. Photobiol., B* **2002**, *66*, 89. (d) Haag, R.; Kratz, F. *Angew. Chem., Int. Ed.* **2006**, *45*, 1198.

(10) Tian, Y. Q.; Watanabe, K.; Kong, X.; Abe, J.; Iyoda, T. *Macromolecules* **2002**, *35*, 3739. (b) Wu, W. C.; Tian, Y. Q.; Chen, C. Y.; Lee, C. S.; Sheng, Y. J.; Chen, W. C.; Jen, A. K.-Y. *Langmuir* **2007**, *23*, 2805. (c) Tian, Y. Q.; Chen, C. Y.; Haller, N. M.; Tucker, N. M.; Ka, J.-W.; Luo, J. D.; Huang, S.; Jen, A. K.-Y. *Macromolecules* **2007**, *40*. (d) Tian, Y. Q.; Chen, C. Y.; Cheng, Y. J.; Young, A. C.; Tucker, N. M.; Jen, A. K.-Y. *Adv. Funct. Mater.* **2007**, *17*, 97. (e) Chen, C.-Y.; Tian, Y. Q.; Cheng, Y.-J.; Young, A. C.; Ka, J.-W.; Jen, A. K.-Y. *J. Am. Chem. Soc.* **2007**, *129*, 7220.

(11) Demas, J. N.; Grosby, G. A. *J. Phys. Chem.* **1971**, *75*, 991.

(12) Seybold, P. G.; Gouterman, M. *J. Mol. Spectrosc.* **1969**, *31*, 1.

(13) Lindsey, J. L.; Wagner, R. W. *J. Org. Chem.* **1989**, *54*, 828.

(14) (a) Wang, J. S.; Matyjaszewski, K. *J. Am. Chem. Soc.* **1995**, *117*, 5614. (b) Ohno, K.; Tsujii, Y.; Fukuda, T. *J. Polym. Sci., Part A: Polym. Chem.* **1998**, *36*, 2473.

(15) Teodorescu, M.; Matyjaszewski, K. *Macromol. Rapid Commun.* **2000**, 190.

(16) (a) Teodorescu, M.; Matyjaszewski, K. *Macromolecules* **1999**, *32*, 4826. (b) Rademacher, J. T.; Baum, M.; Pallack, M. E.; Brittain, W. J.; Simonsick, J. *Macromolecules* **2000**, *33*, 284.

(17) (a) Liu, L.; Niu, Y.; Zhu, X.; Sun, X.; Wang, G.; Jiang, Z. *Colloid Polym. Sci.* **2006**, *284*, 556. (b) Du, W.; Xu, Z.; Nystrom, A. M.; Zhang, K.; Leonard, J. R.; Wooley, K. L. *Bioconjugate Chem.* **2008**, *19*, 2492.

(18) (a) Terreau, O.; Bartels, C.; Eisenberg, A. *Langmuir* **2004**, *20*, 637. (b) Cameron, N. S.; Eisenberg, A.; Brown, G. R. *Biomacromolecules* **2002**, *3*, 124.

(19) (a) Bliznyuk, V. N.; Carter, S. A.; Scott, J. C.; Klaerner, G.; Miller, R. D.; Miller, D. C. *Macromolecules* **1999**, *32*, 361. (b) Teetsov, J.; Fox, M. A. *J. Mater. Chem.* **1999**, *9*, 2117. (c) Lee, J. I.; Klaerner, G.; Miller, R. D. *Chem. Mater.* **1999**, *11*, 1083. (d) Weinfurtner, K. H.; Fujikawa, H.; Tokito, S.; Taga, Y. *Appl. Phys. Lett.* **2000**, *76*, 2502.

(20) Kasha, M. *Radiat. Res.* **1963**, *20*, 55.

(21) The quantum yield of $H_2(Me_3)TPP$ in micelles is 0.0065, which is still lower than that of 0.11 in toluene, showing a possible aggregations of the $H_2(Me_3)TPP$ molecules in the micellar cores.

(22) Energy transfer efficiency was determined by studying the quenching of the donor fluorescence from 400 to 620 nm in the presence of the acceptor at the same excitation wavelength (380 nm). (a) Mugnier, J.; Pouget, J.; Bourson, J.; Valeur, B. *J. Lumin.* **1985**, *33*, 273. (b) Bourson, J.; Mugnier, J.; Valeur, B. *Chem. Phys. Lett.* **1982**, *92*, 430.

(23) For selected reviews, see: (a) Adronov, A.; Fréchet, J. M. J. *Chem. Commun.* **2000**, 1701. (b) Barigelletti, F.; Flamigni, L. *Chem. Soc. Rev.* **2000**, *29*, 1. (c) Choi, M.-S.; Yamazaki, T.; Yamazaki, I.; Aida, T. *Angew. Chem., Int. Ed.* **2004**, *43*, 150.

(24) Lindig, B. A.; Rodger, M. A. J.; Schaap, A. P. *J. Am. Chem. Soc.* **1980**, *102*, 5590.

(25) (a) Lang, K.; Mosinger, J.; Wagnerová, D. M. *Coord. Chem. Rev.* **2004**, *248*, 321. (b) Latch, D. E.; McNeill, K. *Science* **2006**, *311*, 1743.

(26) Tian, N.; Xu, Q.-H. *Adv. Mater.* **2007**, *19*, 1988. (b) Zhang, X.; Xia, Y.; Friend, R. H. *Phys. Rev. B* **2007**, *75*, 245128/1. (c) Wu, C.; Szymanski, C.; Cain, Z.; McNeill, J. *J. Am. Chem. Soc.* **2007**, *129*, 12904.